Supplementary Information for *Relative enrichment of oral bacteria in feces reflects depletion of gut commensals*

LIAO ET AL.

The supplementary material includes **Supplementary Texts**, **Supplementary Figures**, **Supplementary Tables**, and **Supplementary References**.

SUPPLEMENTARY TEXTS

A. Mathematical modeling of intestinal colonization of oral bacteria

A.1. Basic assumptions

Our model is composed of a single compartment (gut lumen) and two coarse-grained bacterial populations: (1) bacteria transmitted from the oral cavity (B_o) and (2) gut resident bacteria (B_g). Host effects such as gut inflammation are not explicitly modeled. We consider the following ecological-environmental processes shaping the dynamics of the two populations:

- Arrival of live oral bacteria to the gut lumen follows a zero-order process with the constant rate α_o. Since oral cavity would be only briefly exposed to antibiotics during swallowing [1], we assume that antibiotics do not affect α_o;
- Loss of oral and gut bacteria (e.g., death, fecal excretion) follow first-order kinetics with the rate constant δ. Antibiotics may induce diarrhea but this effect is indirect and generally mild [2]. We assume that antibiotics do not affect δ;
- Proliferation of both gut and oral bacteria follow logistic growth with maximum proliferation rates (γ_o and γ_g) and a saturation term that specifies the maximal load (i.e., carrying capacity) of oral (K_o) and gut (K_g) bacteria. Antibiotics reduce the maximum growth rates of both populations and the reduction levels are quantified by ϵ_o and ϵ_g (both range between 0 and 1) for oral and gut bacteria respectively.

A.2. Analytical solutions

There are two solutions of this model at steady state (i.e., $d[B_o]/dt = d[B_g]/dt = 0$). The trivial solution is given by (subscript *ss* indicates steady state solution)

$$[B_o]_{ss,1} = \frac{K_o(\gamma_o\epsilon_o - \delta) + \sqrt{K_o^2(\delta - \gamma_o\epsilon_o)^2 + 4\alpha_o\gamma_o\epsilon_o K_o}}{2\gamma_o\epsilon_o} \quad \text{(S1)}$$

$$[B_g]_{ss,1} = 0 \quad \text{(S2)}$$

and the non-trivial solution is given by

$$[B_o]_{ss,2} = \frac{\alpha_o}{\delta\left(1 - \frac{\gamma_o\epsilon_o}{\gamma_g\epsilon_g}\right)} \quad \text{(S3)}$$

$$[B_g]_{ss,2} = K_g\left(1 - \frac{\delta}{\gamma_g\epsilon_g}\right) - \frac{\alpha_o K_g}{\delta K_o\left(1 - \frac{\gamma_o\epsilon_o}{\gamma_g\epsilon_g}\right)} \quad \text{(S4)}$$

Note that $[B_o]_{ss,1}$ is non-negative regardless of the parameter values so the trivial solution always exists. However, either or both of $[B_o]_{ss,2}$ and $[B_g]_{ss,2}$ can be negative for specific combinations of parameter values. In these scenarios, the nontrivial solution does not exist and the steady state always converges to the trivial solution. Instead, the differential equation will converge to the nontrivial solution when it exists because the trivial solution is then unstable.

Combining Eqs. (S1)-(S4) gives the relative abundance of oral bacteria ($f_o(\epsilon_o, \epsilon_g) = [B_o]/([B_o] + [B_g])$) and total bacterial load ($L(\epsilon_o, \epsilon_g) = [B_o] + [B_g]$), whose expressions are shown below

$$f_o(\epsilon_o, \epsilon_g) = \begin{cases} 1 & \text{trivial} \\ \dfrac{1}{1 - \dfrac{K_g}{K_o} + \dfrac{\delta K_g \left(1 - \dfrac{\delta}{\gamma_g \epsilon_g}\right)\left(1 - \dfrac{\gamma_o \epsilon_o}{\gamma_g \epsilon_g}\right)}{\alpha_o}} & \text{nontrivial} \end{cases} \tag{S5}$$

$$L(\epsilon_o, \epsilon_g) = \begin{cases} \dfrac{K_o(\gamma_o \epsilon_o - \delta) + \sqrt{K_o^2(\delta - \gamma_o \epsilon_o)^2 + 4\alpha_o \gamma_o \epsilon_o K_o}}{2\gamma_o \epsilon_o} & \text{trivial} \\ \dfrac{\alpha_o(1 - K_g/K_o)}{\delta\left(1 - \dfrac{\gamma_o \epsilon_o}{\gamma_g \epsilon_g}\right)} + K_g\left(1 - \dfrac{\delta}{\gamma_g \epsilon_g}\right) & \text{nontrivial} \end{cases} \tag{S6}$$

B. Parameter estimation

B.1. Theoretical modeling: γ_o and γ_g

We retrieved species-level relative abundance profiles of paired fecal and oral cavity samples of the Human Microbiome Project (HMP) [3] (414 oral cavity samples from multiple subsites and 147 fecal samples) and Brito et al. [4] (140 saliva samples and 172 fecal samples) using the *curatedMetagenomicData* package [5]. We then identified 92 bacterial species (Table S6) typical of the oral cavity by using the following filtering criteria: the mean relative abundance and prevalence (at a presence cutoff of 10^{-3}) of the species across all oral cavity samples must be greater than 0.1% and 5% respectively, and their values across all fecal samples must be no greater than the same thresholds. Using the list, we found that 60 out of 818 bacterial genomes with genome-scale metabolic models in the Virtual Metabolic Human Database [6] belong to oral bacteria. The values of γ_o and γ_g were estimated by simulating the maximum growth rates of oral and gut bacterial species under the western diet using flux balance analysis [7]. The mean specific growth rate over 60 oral and 758 gut bacterial genomes are $\gamma_o = 0.24\ [1/hr]$ and $\gamma_g = 0.35\ [1/hr]$ respectively. This computational result is consistent with our expectation that the gut bacteria grow faster in the environment they are associated with.

B.2. Literature values: K_g and δ

The intestinal carrying capacity for the gut bacteria can be estimated from fecal bacterial density in healthy people, where the fraction of oral bacteria is relatively minor and can be ignored. According to Achour et al. [8], the average stool wet weight is 150 $[g/day]$ in which bacteria contribute 19 $[g/day]$ dry weight. Given that the density of human feces is 1.06 $[g/mL]$ [9] and the average mass of a bacterium is 4.6×10^{-12} $[g]$ [10], a typical value of K_g is equal to $19/(4.6 \times 10^{-12})/(150/1.06) = 2.92 \times 10^{10}\ [cells/mL]$.

The rate of bacterial loss in the absence of antibiotic treatment is mainly determined by colon transit time: we used $\delta = 0.08\ [1/hr]$, the dilution rate used to establish a 48-hr colon transit time *in vitro* in a chemostat for the simulation

of human intestinal microbiota [11]. We ignored the natural death rate as it is at least one order of magnitude lower (typically on the order of 10^{-4}-10^{-3} per hour [12–14]).

B.3. Fitting human data: K_o and α

We employed the same cohort of allo-HCT recipients as described in Fig. 4 of the main text to estimate the intestinal carrying capacity for the oral bacteria. The allo-HCT cohort was selected for data fitting because the microbiome compositions of these patients were enriched with oral bacteria at varying levels (Fig. 4A). From the cohort, we first identified all patients who contained at least one post-antibiotic fecal sample with relative abundance of oral bacteria exceeding a threshold (30%, 40%, 50%, 60% and 70%). The samples for parameter estimation include all collected on days prior to or after antibiotic administration and also measured by qPCR for the total bacterial loads among these patients. The values of K_o and K_g were obtained by solving the following series of overdetermined linear equations

$$\frac{Q_i f_{o,i}}{K_o} + \frac{Q_i(1-f_{i,2})}{K_g} = 1 \tag{S7}$$

where i represents each sample, Q_i represents the qPCR value of the sample i, and $f_{o,i}$ represents the oral bacterial fraction of the sample i. By constructing the linear equations, we implicitly assumed that the gut environments of allo-HCT recipients have reached their 100% carrying capacity for oral and gut bacteria together. This assumption may not be universally satisfied but should be sufficient to estimate the correct order-of-magnitude for the ratio between K_o and K_g. The ratio was robust when we varied the threshold for patient inclusion and equals to 11.81, 14.64, 17.54, 14.43 and 16.77 for 30%, 40%, 50%, 60% and 70% respectively. Using their average (15.04) for K_g/K_o, the corresponding estimate of K_o is given by 1.94×10^9 $(= 2.92 \times 10^{10}/15.04)$ $[cells/mL]$.

Given the values of all other parameters (γ_o, γ_g, K_g, K_o, δ), the arrival rate of live oral bacteria to the gut (α_o) was estimated to be equal to 3.10×10^5 $[1/hr/mL]$ by requiring the simulated oral bacterial fraction in the absence of antibiotics equals to the value averaged across all HMP healthy subjects (0.05%). On average, we humans swallow 1.5×10^{12} oral bacteria in 1.5 $[L]$ saliva per day [15] and the estimated transmission rate of all live and dead oral bacteria is equal to $1.5 \times 10^{12}/24/1.5 \times 10^3 = 4.2 \times 10^7$ $[1/hr/ml]$. This indicates that only 0.74% oral bacteria can reach human gut alive while the others may be killed during the passage through the gastrointestinal tract.

C. Justification of using qPCR for oral bacterial quantification

Suppose a fecal sample contains live bacteria translocated from the oral cavity (relative abundance x), live gut-resident bacteria (relative abundance y), and other DNAs from dead cells (including free DNAs, relative abundance $1-x-y$). If the total load of all live bacteria (absolute abundance) is L^{live}, the load of all live oral bacteria in feces is $L^{live}x/(x+y)$. Note that the oral bacterial fraction estimated by 16S rRNA sequencing is $f_o^{16S} = x$ because all DNAs from live and dead cells were mixed in the sequencer. Correspondingly, the qPCR-based total bacterial loads is given by $L^{qPCR} = L^{live}/(x+y)$. It can be easily shown

that qPCR-based quantification preserves the absolute abundance of live oral bacteria, i.e., $L^{qPCR} f_o^{16S} = L^{live} x/(x+y)$.

SUPPLEMENTARY FIGURES

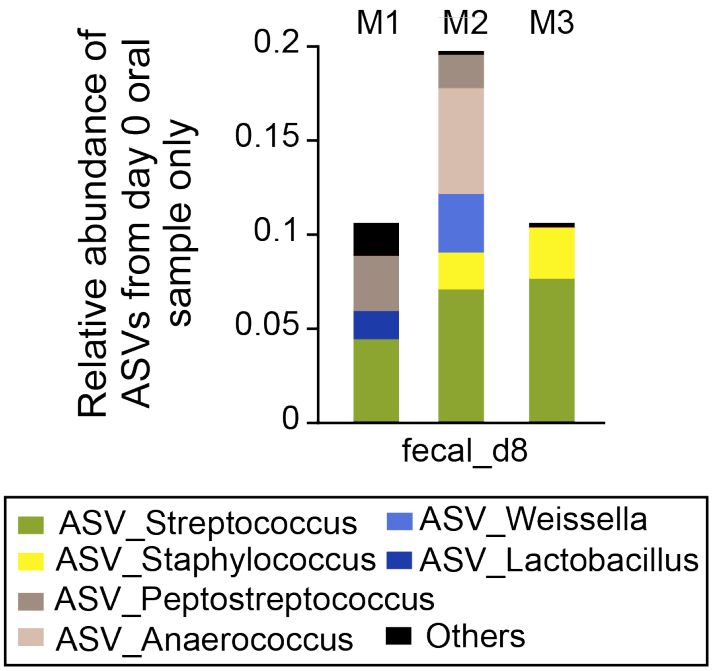

Fig. S1. (Related to Fig. 2) Taxonomy of ASVs in the post-treatment fecal samples that were only found in the pre-treatment oral samples of the same mice. M1, M2, and M3 represent three mice. fecal_d8: post-treatment fecal sample on day 8.

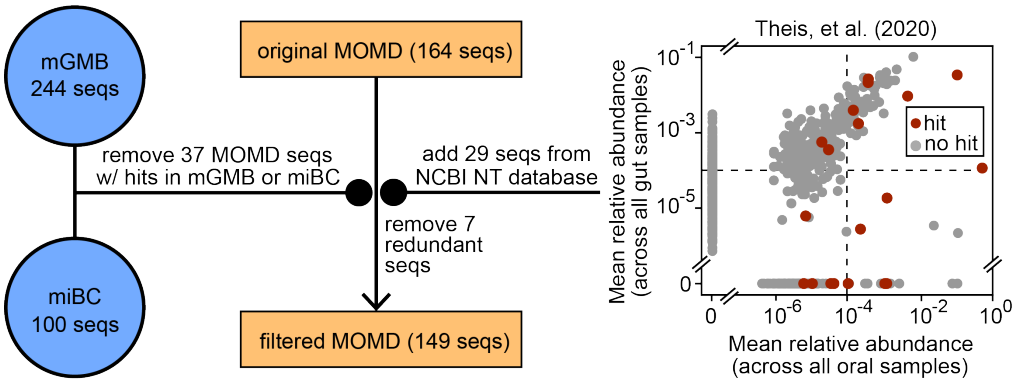

Fig. S2. (Related to Fig. 2) Schematic diagram of the method for constructing a reference set of oral bacterial 16S rRNA sequences in mouse. Briefly, we removed sequences that are cultivable in the mouse gut from the original MOMD (Mouse Oral Microbiome Database [16]) and added new oral-typical sequences identified from a public study (Theis, et al., (2020)) [17] but missed in MOMD. In the scatter plot, hits refer to amplicon sequence variants matching at least one sequence in MOMD. mGMB: the mouse Gut Microbial Biobank [18]; miBC: the mouse intestinal Bacterial Collection [19]; Seqs: sequences. See STAR Methods of the main text for details.

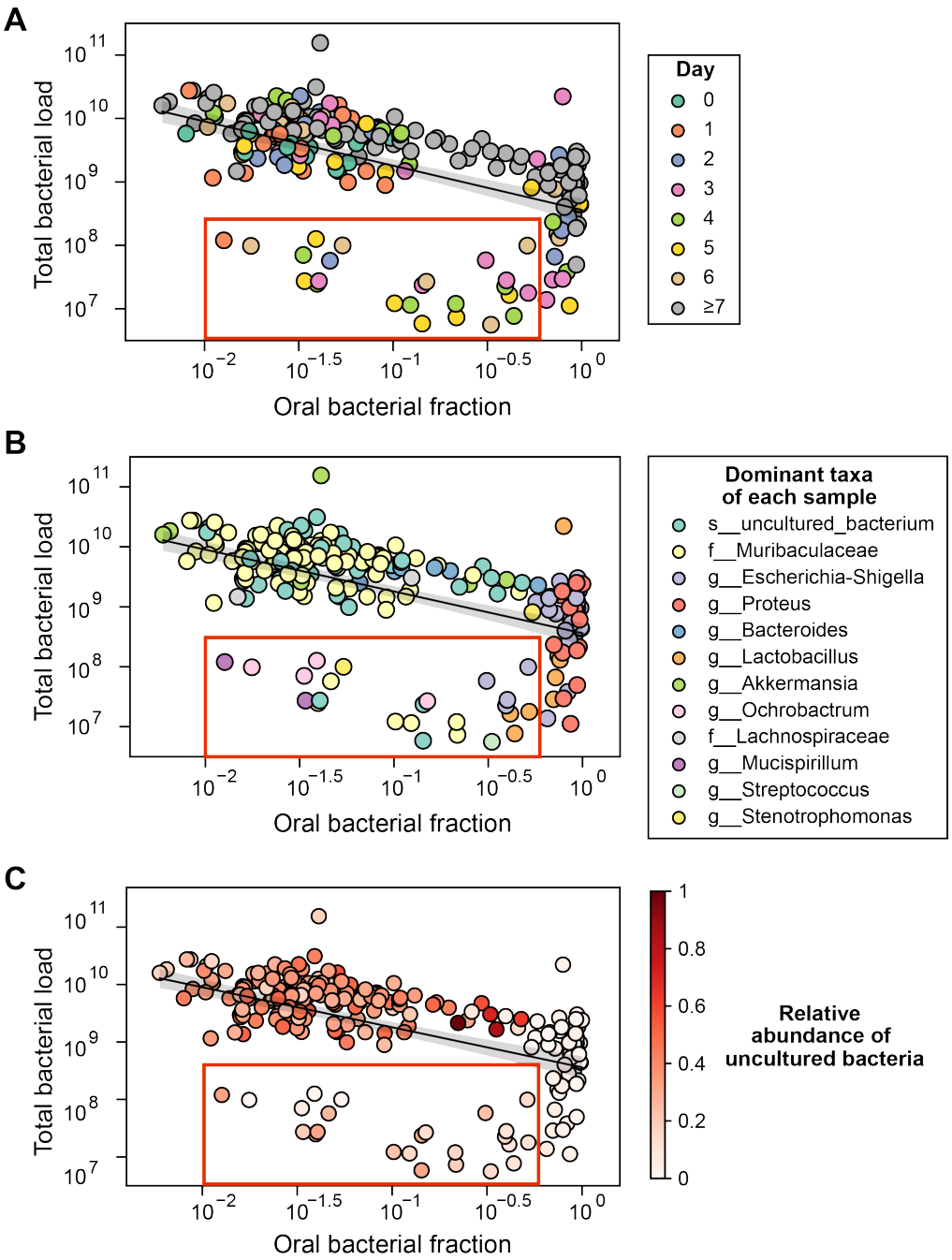

Fig. S3. (Related to Fig. 2) The same plot as Fig. 2J of the main text but colored by (**A**) the day of sample collection, (**B**) the most abundance taxa (grouped at the lowest classified level), and (**C**) the relative abundance of uncultured bacteria. The red box (oral bacterial fraction $\leq 10^{-0.25}$ and total bacterial load $\leq 10^8$ 16S copies per gram feces) encloses outlier samples deviated from the black trend line.

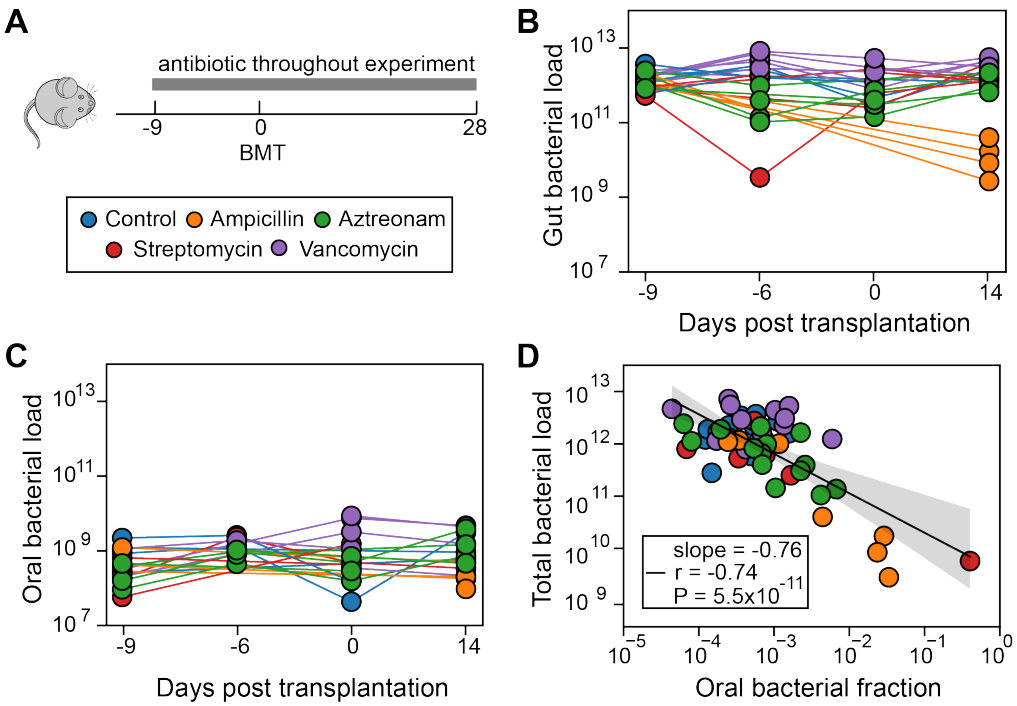

Fig. S4. (Related to Fig. 2) Additional mouse experiments [20] showing that the oral bacterial loads in the gut remain stable under antibiotic treatment. (**A**) Experiment design. Mice were given a split 1100cGy radiation dose and administered 5×10^6 bone marrow cells via tail vein injection at day 0. Ampicillin, aztreonam, streptomycin and vancomycin were started 9 days before bone marrow transplantation (BMT) and administered throughout the experiment. Except for ampicillin (4 mice), all other antibiotic treatments (including the control group) were repeated in 5 mice. (**B, C**) Dynamics of gut bacterial loads (B) and oral bacterial loads (C) during BMT. Each trajectory represents a mouse. (**D**) Linear relationship between oral bacterial fractions and total bacterial loads in the log-log space. Black line: best linear fit; shading: 95% confidence interval. Unit of bacterial loads: 16S copies per gram feces.

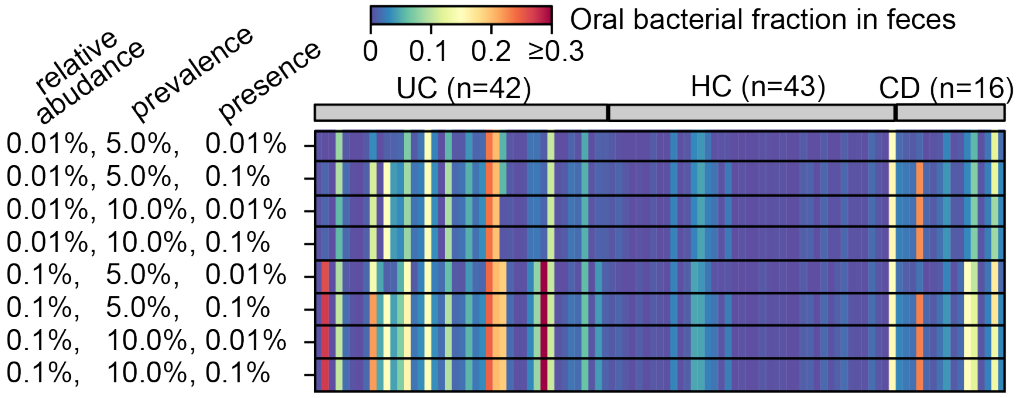

Fig. S5. (Related to Fig. 3) Effects of filtering thresholds on the estimation of oral bacterial fractions in the feces of the IBD cohort shown in Fig. 3 of the main text. We varied the thresholds of mean relative abundance (0.01%, 0.1%), prevalence (5%, 10%), and the definition of ASV presence (0.01%, 0.1%) in the computation of prevalence to select for ASVs typical of the oral cavity from the Human Microbiome Project. The oral bacterial fractions formed vertical colored bands in the heatmap, suggesting that they are largely insensitive to the variations in filtering thresholds. CD: Crohn's disease; UC: ulcerative colitis; HC: healthy controls.

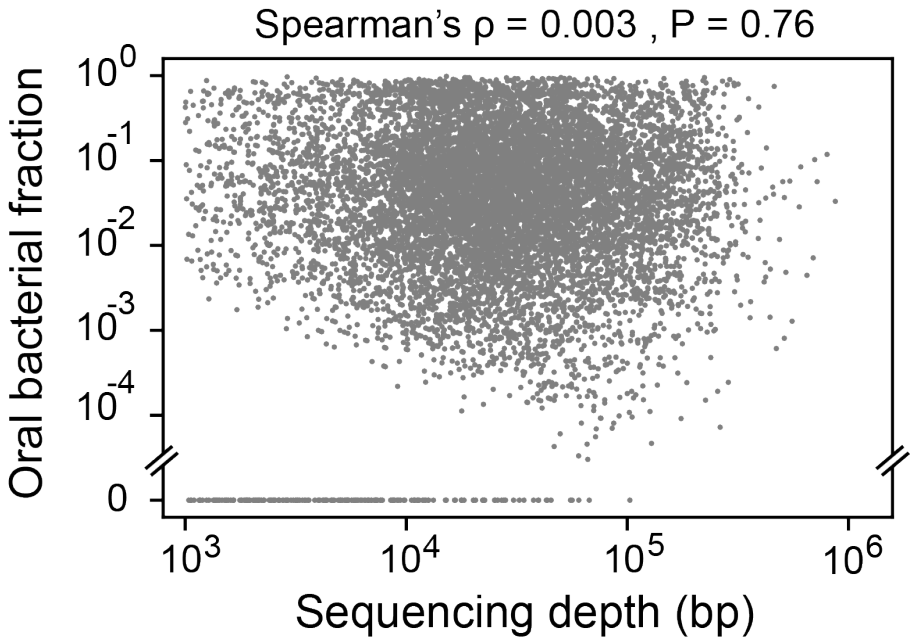

Fig. S6. (Related to Fig. 4) Total fractions of oral bacteria are not associated with sequencing depths across fecal samples of the same allo-HCT (allogeneic hematopoietic cell transplantation) recipients shown in Fig. 4 of the main text.

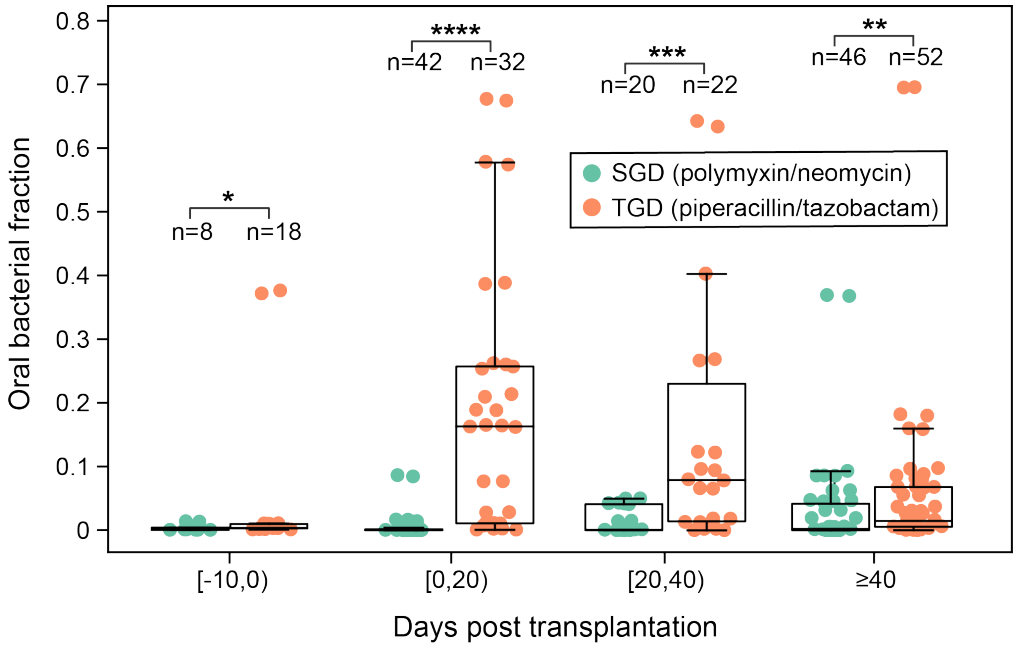

Fig. S7. (Related to Fig. 4) Piperacillin/tazobactam (TZP) caused significant enrichment of oral bacteria in the feces of 19 pediatric allo-HCT (allogeneic hematopoietic cell transplantation) recipients (1-17 year old, 10.1 year old on average) [21]. Samples were grouped into four different stages of transplantation. TZP was used in total gut decontamination (TGD) as the only antibacterial antibiotic, while polymycin/neomycin was used in selective gut decontamination (SGD). The administration of SGD and TGD started 10 days before transplantation until engraftment or 21 days after transplantation, whichever occurred later. The comparison is visualized using box plot overlaid on top of a strip plot (each dot represents one sample), with central line representing the median, box limits representing the first and third quartiles, and whiskers extending to the smallest and largest values or at most to 1.5× the interquartile range, whichever is smaller. ****, P<0.0001; ***, P<0.001, **, P<0.01; *, P<0.05. Kruskal-Wallis test.

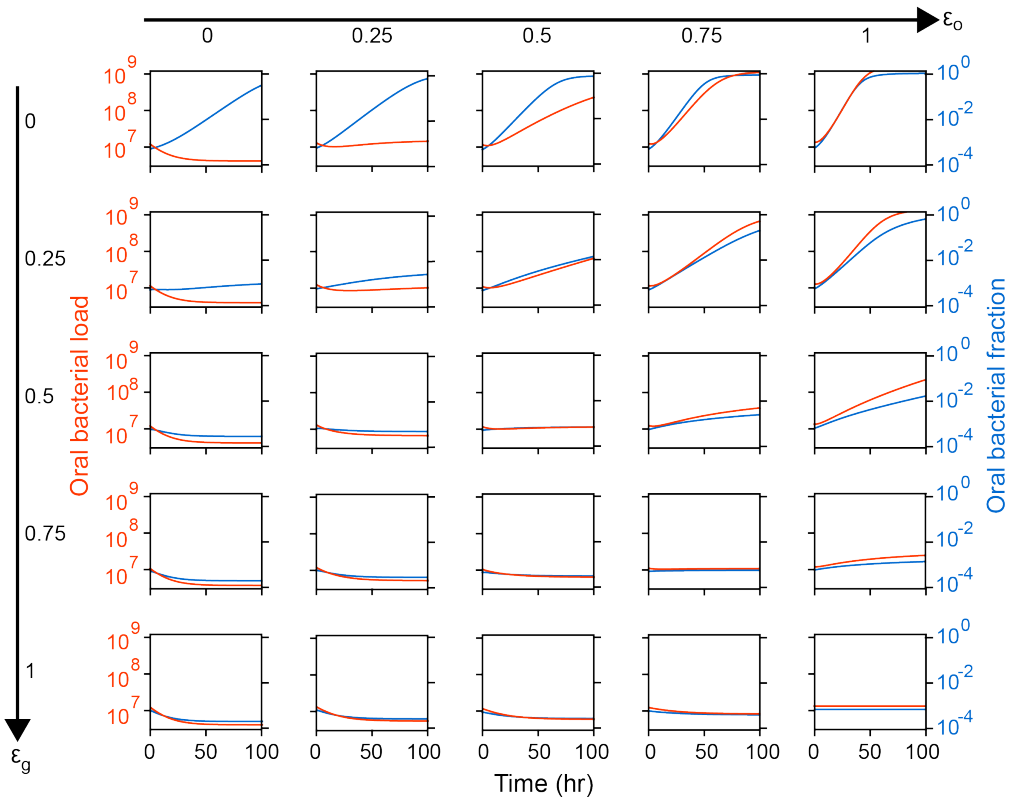

Fig. S8. (Related to Fig. 5) Simulated relative (blue) and absolute (orange) abundances of oral bacterial populations in the human gut under constant antibiotic exposure. The antibiotic susceptibility parameters of gut (ϵ_g) and oral (ϵ_o) bacteria were varied on a 2D grid. Unit of oral bacterial load: 16S copies per gram feces.

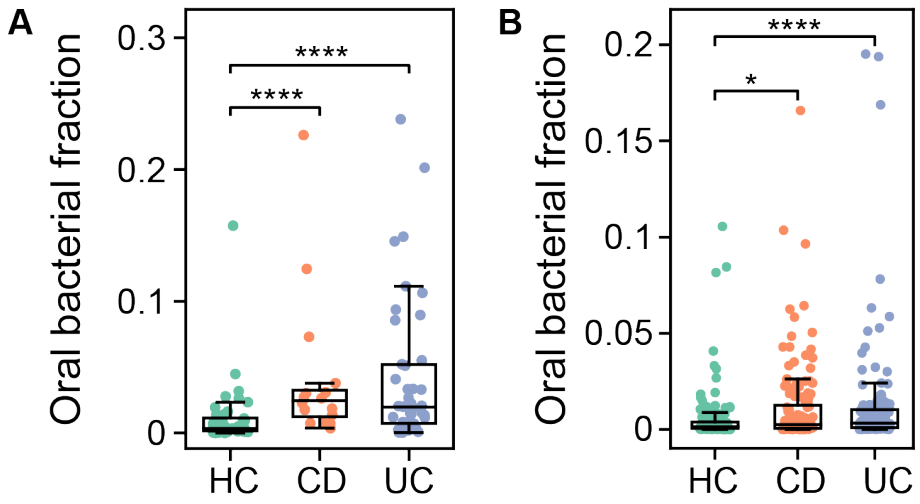

Fig. S9. (Related to Fig. 6) Oral bacteria showed significantly higher enrichment in the feces of patients with Crohn's disease (CD) and ulcerative colitis (UC) compared to their healthy controls (HC). (**A**) Imai et al. [22]. Participants who took any antibiotics within the last 3 months were excluded. (**B**) Pascal et al. [23]. Participants who were treated by antibiotics within the previous 4 weeks were excluded. The comparison is visualized using box plot overlaid on top of a strip plot (each dot represents one sample), with central line representing the median, box limits representing the first and third quartiles, and whiskers extending to the smallest and largest values or at most to 1.5× the interquartile range, whichever is smaller. ****, P<0.0001; *, P<0.05. Kruskal-Wallis test.

SUPPLEMENTARY TABLES

Parameter	Value	Description
α_o	3.10×10^5 $[1/hr/mL]$	transmission rate of oral bacteria to human gut
γ_o	0.24 $[1/hr]$	maximum growth rate of oral bacteria in human gut
γ_g	0.35 $[1/hr]$	maximum growth rate of gut bacteria in human gut
K_o	1.94×10^9 $[cells/mL]$	intestinal carrying capacity for oral bacterial populations
K_g	2.92×10^{10} $[cells/mL]$	intestinal carrying capacity for gut bacterial populations
δ	0.08 $[1/hr]$	rate constant of bacterial loss

Table S5. Default values of model parameters.

SUPPLEMENTARY REFERENCES

1. V. R. Carr, E. A. Witherden, S. Lee, S. Shoaie, P. Mullany, G. B. Proctor, D. Gomez-Cabrero, and D. L. Moyes, "Abundance and diversity of resistomes differ between healthy human oral cavities and gut," Nat. communications **11**, 1–10 (2020).
2. C. R. Polage, J. V. Solnick, and S. H. Cohen, "Nosocomial diarrhea: evaluation and treatment of causes other than *Clostridium difficile*," Clin. Infect. Dis. **55**, 982–989 (2012).
3. The Human Microbiome Project Consortium, "Structure, function and diversity of the healthy human microbiome," Nature **486**, 207–214 (2012).
4. I. L. Brito, S. Yilmaz, K. Huang, L. Xu, S. D. Jupiter, A. P. Jenkins, W. Naisilisili, M. Tamminen, C. Smillie, J. R. Wortman *et al.*, "Mobile genes in the human microbiome are structured from global to individual scales," Nature **535**, 435–439 (2016).
5. E. Pasolli, L. Schiffer, P. Manghi, A. Renson, V. Obenchain, D. T. Truong, F. Beghini, F. Malik, M. Ramos, J. B. Dowd *et al.*, "Accessible, curated metagenomic data through ExperimentHub," Nat. Methods **14**, 1023–1024 (2017).
6. A. Noronha, J. Modamio, Y. Jarosz, E. Guerard, N. Sompairac, G. Preciat, A. D. Daníelsdóttir, M. Krecke, D. Merten, H. S. Haraldsdóttir *et al.*, "The Virtual Metabolic Human database: integrating human and gut microbiome metabolism with nutrition and disease," Nucleic Acids Res. **47**, D614–D624 (2019).
7. J. D. Orth, I. Thiele, and B. Ø. Palsson, "What is flux balance analysis?" Nat. Biotechnol. **28**, 245–248 (2010).
8. L. Achour, S. Nancey, D. Moussata, I. Graber, B. Messing, and B. Flourie, "Faecal bacterial mass and energetic losses in healthy humans and patients with a short bowel syndrome," Eur. J. Clin. Nutr. **61**, 233–238 (2007).
9. D. Brown, D. Butler, N. Orman, and J. Davies, "Gross solids transport in small diameter sewers," Water Sci. Technol. **33**, 25–30 (1996).
10. A. M. Stephen and J. Cummings, "The microbial contribution to human faecal mass," J. Med. Microbiol. **13**, 45–56 (1980).
11. W. Tottey, D. Feria-Gervasio, N. Gaci, B. Laillet, E. Pujos, J.-F. Martin, J.-L. Sebedio, B. Sion, J.-F. Jarrige, M. Alric *et al.*, "Colonic transit time is a driven force of the gut microbiota composition and metabolism: in vitro evidence," J. Neurogastroenterol. Motil. **23**, 124 (2017).
12. T. T. Nguyen, J. Guedj, E. Chachaty, J. de Gunzburg, A. Andremont, and F. Mentré, "Mathematical modeling of bacterial kinetics to predict the impact of antibiotic colonic exposure and treatment duration on the amount of resistant enterobacteria excreted," PLoS Comput. Biol. **10**, e1003840 (2014).
13. C. Spalding, E. Keen, D. J. Smith, A.-M. Krachler, and S. Jabbari, "Mathematical modelling of the antibiotic-induced morphological transition of *Pseudomonas aeruginosa*," PLoS Comput. Biol. **14**, e1006012 (2018).
14. S. J. Schink, E. Biselli, C. Ammar, and U. Gerland, "Death rate of *E. coli* during starvation is set by maintenance cost and biomass recycling," Cell

Syst. **9**, 64–73 (2019).
15. T. S. Schmidt, M. R. Hayward, L. P. Coelho, S. S. Li, P. I. Costea, A. Y. Voigt, J. Wirbel, O. M. Maistrenko, R. J. Alves, E. Bergsten *et al.*, "Extensive transmission of microbes along the gastrointestinal tract," Elife **8**, e42693 (2019).
16. S. Joseph, J. Aduse-Opoku, A. Hashim, E. Hanski, R. Streich, S. C. Knowles, A. B. Pedersen, W. G. Wade, and M. A. Curtis, "A 16s rrna gene and draft genome database for the murine oral bacterial community," Msystems **6**, e01222–20 (2021).
17. K. R. Theis, R. Romero, J. M. Greenberg, A. D. Winters, V. Garcia-Flores, K. Motomura, M. M. Ahmad, J. Galaz, M. Arenas-Hernandez, and N. Gomez-Lopez, "No consistent evidence for microbiota in murine placental and fetal tissues," Msphere **5**, e00933–19 (2020).
18. C. Liu, N. Zhou, M.-X. Du, Y.-T. Sun, K. Wang, Y.-J. Wang, D.-H. Li, H.-Y. Yu, Y. Song, B.-B. Bai *et al.*, "The mouse gut microbial biobank expands the coverage of cultured bacteria," Nat. communications **11**, 1–12 (2020).
19. I. Lagkouvardos, R. Pukall, B. Abt, B. U. Foesel, J. P. Meier-Kolthoff, N. Kumar, A. Bresciani, I. Martínez, S. Just, C. Ziegler *et al.*, "The mouse intestinal bacterial collection (mibc) provides host-specific insight into cultured diversity and functional potential of the gut microbiota," Nat. microbiology **1**, 1–15 (2016).
20. A. Staffas, M. B. da Silva, A. E. Slingerland, A. Lazrak, C. J. Bare, C. D. Holman, M. D. Docampo, Y. Shono, B. Durham, A. J. Pickard *et al.*, "Nutritional support from the intestinal microbiota improves hematopoietic reconstitution after bone marrow transplantation in mice," Cell Host & Microbe **23**, 447–457 (2018).
21. V. Bekker, R. D. Zwittink, C. W. Knetsch, I. M. Sanders, D. Berghuis, P. J. Heidt, J. M. Vossen, W. M. de Vos, C. Belzer, R. G. Bredius *et al.*, "Dynamics of the gut microbiota in children receiving selective or total gut decontamination treatment during hematopoietic stem cell transplantation," Biol. Blood Marrow Transplantation **25**, 1164–1171 (2019).
22. J. Imai, H. Ichikawa, S. Kitamoto, J. L. Golob, M. Kaneko, J. Nagata, M. Takahashi, M. G. Gillilland III, R. Tanaka, H. Nagao-Kitamoto *et al.*, "A potential pathogenic association between periodontal disease and Crohn's disease," JCI Insight **6** (2021).
23. V. Pascal, M. Pozuelo, N. Borruel, F. Casellas, D. Campos, A. Santiago, X. Martinez, E. Varela, G. Sarrabayrouse, K. Machiels *et al.*, "A microbial signature for Crohn's disease," Gut **66**, 813–822 (2017).